Origin of the Enhanced Copper Spin Echo Decay Rate in the Pseudogap Regime of the Multilayer High-T_c Cuprates

Atsushi Goto,[1,2] W. G. Clark,[1] Patrik Vonlanthen,[1] Kenji B. Tanaka,[1] Tadashi Shimizu,[2] Kenjiro Hashi,[2]
P. V. P. S. S. Sastry,[3,4] and Justin Schwartz[3,4]

[1]*Department of Physics and Astronomy, University of California, Los Angeles, California 90095-1547*
[2]*National Institute for Materials Science, 3-13, Sakura, Tsukuba, Ibaraki, 305-0003, Japan*
[3]*National High Magnetic Field Laboratory, 1800 E. Paul Dirac Drive, Tallahassee, Florida 32310*
[4]*Department of Mechanical Engineering, FAMU-FSU College of Engineering, Tallahassee, Florida 32306*

We report measurements of the anisotropy of the spin echo decay for the inner layer Cu site of the triple layer cuprate $Hg_{0.8}Re_{0.2}Ba_2Ca_2Cu_3O_8$ ($T_c = 126$ K). The angular dependence of the second moment ($T_{2M}^{-2} \equiv \langle \Delta\omega^2 \rangle$) deduced from the decay curves indicates that T_{2M}^{-2} for $H_0 \parallel$ c is enhanced in the pseudogap regime below $T_{pg} \sim 170$ K, as seen in bilayer systems. Comparison of T_{2M}^{-2} between $H_0 \parallel$ c and $H_0 \perp$ c indicates that this enhancement is caused by electron spin correlations between the inner and the outer CuO_2 layers. The results provide the answer to the long-standing controversy regarding the opposite T dependences of $(T_1 T)^{-1}$ and T_{2G}^{-2} (T_{2G}: Gaussian component) in the pseudogap regime of multilayer systems.

NMR has greatly contributed to the understanding of the pseudogap phenomenon observed in the anomalous normal states of high-T_c cuprates, but there still remain some important issues to be resolved. One is the temperature (T) dependence of the spin-lattice relaxation time (T_1) and the Gaussian component of the spin-spin relaxation time (T_{2G}). In systems such as $YBa_2Cu_3O_{6.6}$ and $YBa_2Cu_4O_8$, T_{2G}^{-2} continues to grow as T is lowered towards T_c, whereas $(T_1 T)^{-1}$ decreases in the pseudogap regime [1,2]. If the same dynamical susceptibility $\chi(\mathbf{q}, \omega)$ is responsible for both relaxation rates, an *anomalous* enhancement should occur at the high frequency part of $Im\chi(\mathbf{q}, \omega)$ that is greater than that caused by the transfer of spectral weight from the low frequency part. Although this behavior is expected in the *real* spin gap states of insulators [3–5], it appears abnormal for the pseudogap states in metals [6]. This issue has puzzled theorists [7–9], and other explanations have been sought.

A key to resolve the problem is that the phenomenon is observed only in multilayer systems. Simultaneous decreases of $(T_1 T)^{-1}$ and T_{2G}^{-2} are observed in a single layer system [10]. One proposed mechanism for multilayer systems is spin correlations between adjacent layers [11–13], which had been observed in spin echo double resonance (SEDOR) experiments [14,15]. In bilayer systems, the two CuO_2 layers in a unit cell are equivalent, so that the Cu nuclei on one of the layers behave as like-spins to the others in the echo decay process and contribute to T_{2G}^{-2} through the interlayer spin correlations. Unfortunately, since the contribution from the interlayer coupling is indistinguishable from its intralayer counterpart for the identical layers, it is difficult to extract the effect experimentally in such systems.

In order to identify experimentally the interlayer effects on T_{2G}, we have utilized the trilayer cuprate $Hg_{0.8}Re_{0.2}Ba_2Ca_2Cu_3O_8$ ($T_c = 126$ K) with a pseudogap ($T_{pg} \sim 170$ K), where one inner and two outer CuO_2 layers are crystallographically inequivalent. This enables us to separate the interlayer effects from the total decay rates. In this Letter, we report the measurements of the angular dependence of the second moment in the inner Cu site, which identifies the role of interlayer correlations in the echo decay process in the pseudogap regime of a multilayer system. Our analysis of the results shows that the different behavior of $(T_1 T)^{-1}$ and T_{2G}^{-2} is caused by interlayer spin correlations, and that an *anomalous* enhancement of $Im\chi(\mathbf{q}, \omega)$ is not needed to account for it.

The powder sample was prepared using the method of Ref. [16] and magnetically oriented along the c axis. Figure 1 shows the angular dependence of the frequency spectrum for the ^{63}Cu central transition at 135 K and $H_0 = 9.0$ T. The angle θ is that between H_0 and the c axis. Each curve was obtained by adding the real part of the Fourier transform (FT) spectra of the half echo measured at a few different frequencies [17]. The relatively narrow and wide lines are assigned to Cu(1) and Cu(2) sites in the inner and outer layers, respectively [18]. We confirmed that K_s and the quadrupole frequency (ν_Q) are consistent with previous results [19,20]. The triangles in Fig. 1 indicate the positions at which echo decays were measured. Since the Cu(1) and Cu(2) lines overlap at 10° and 70°, both lines contribute to the measured decay.

The angular dependence of the echo decay curves at 135 K is shown in Fig. 2(a), where the Redfield contribution from T_1 has been removed by dividing the measured data by $\exp(-2\tau/T_{1R})$ [21] with T_{1R} obtained as follows [22]. The general form of T_{1R}^{-1} is given by

$$(T_{1R})_z^{-1} = \{I(I+1) - 1/4\}(W_x + W_y) + W_z, \quad (1)$$
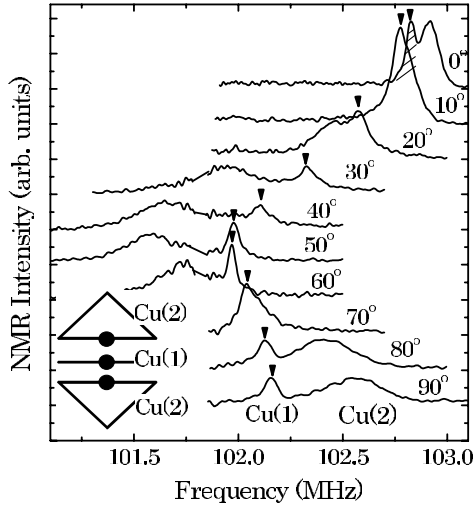
FIG. 1. Absorption spectra for the central transition of ^{63}Cu at 135 K and $H_0 = 9.0$ T as a function of θ. The triangles show the part of the spectra used for the T_2 measurements. Inset: Schematic view of the CuO$_2$ layers.

FIG. 2 (color online). Angular dependences of (a) the echo decay curve, (b) $(T_1 T)^{-1}$, (c) T_{2G}^{-1} (•) and T_{2L}^{-1} (△) in Eq. (3), and (d) T_{2M}^{-2} deduced from T_{2G}^{-2} (•) and T_{2L}^{-2} (△) at 135 K. The dashed curve in (d) is given by Eq. (9).

where W_γ ($\gamma = x, y, z$) is from the spin fluctuations in the γ direction and z is the quantization axis ($\parallel H_0$). In the same notation, $(T_1)_z^{-1}$ is given by $(T_1)_z^{-1} = W_x + W_y$. Hence, for an arbitrary θ,

$$[T_{1R}(\theta)]^{-1} = \{I(I+1) - 1/4\}[T_1(\theta)]^{-1} \\ + [T_1(90° - \theta)]^{-1} - 0.5[T_1(0°)]^{-1}, \quad (2)$$

where the relation $W_a = W_b$ is used (the subscripts a, b correspond to the crystalline axes). From the anisotropy of $(T_1 T)^{-1}$ in Fig. 2(b), $[T_{1R}(\theta)]^{-1}$ is calculated.

Figure 2(a) shows that the shape of the decay curve changes from Gaussian at 0° to single exponential (Lorentzian spectrum) at 90°. These data are fitted by the function

$$\frac{M(2\tau)}{e^{-2\tau/T_{1R}}} = M_0 \exp\left[-\frac{2\tau}{T_{2L}} - \frac{1}{2}\left(\frac{2\tau}{T_{2G}}\right)^2 \right] \quad (3)$$

with M_0, T_{2L}, and T_{2G} as free parameters. The angular dependences of T_{2L}^{-1} and T_{2G}^{-1} thus obtained are shown in Fig. 2(c). For 0° ∼ 20°, T_{2L}^{-1} is nearly zero while T_{2G}^{-1} is zero at 80° and 90°. In between, the decay curve crosses over between these two extremes. This change is a result of the NMR line narrowing caused by the following mechanism. At finite T the effective interaction between adjacent nuclear spins is reduced because of rapid spin flips driven by the hyperfine interaction with the electrons, which averages out the nuclear fields at adjacent nuclear sites. As a result, the central part of the NMR line is narrowed and the spectrum approaches a Lorentzian rather than a Gaussian shape [22–24]. The importance of the effect depends on the ratio between the two time scales T_1 and $T_{2M} \equiv \langle \Delta\omega^2 \rangle^{-1/2}$, where $\langle \Delta\omega^2 \rangle$ is the homogeneous second moment of the NMR absorption.

The former and the latter characterize the time scales of the nuclear spin fluctuations and the echo decays, respectively.

There are two limiting cases where analytical forms for the decays are known. One is the static limit ($T_1/T_{2M} \gg 1$), where nuclear spins do not change their states between pulses or a pulse and an echo because of the relatively long T_1. Consequently, the contributions from unlike-spins are canceled out at the time of the echo and only like-spins contribute to the echo decay. The decay in this case is described by a Gaussian [1],

$$\frac{M(2\tau)}{e^{-2\tau/T_{1R}}} = M_0 \exp\left[-\frac{1}{2}\left(\frac{2\tau}{T_{2M}}\right)^2 \right] f(2\tau), \quad (4)$$

where $f(2\tau)$ is the correction for the narrowing effect [24,25] and in the static limit, $f(2\tau) \equiv 1$. The rate T_{2M}^{-1} in this case is usually referred to as the Gaussian rate, T_{2G}^{-1}.

The second is the narrowed limit ($T_1/T_{2M} \lesssim 1$), where nuclei are fluctuating during the echo sequence. The decay is characterized by a single exponential (Lorentzian spectrum) [22–24],

$$\frac{M(2\tau)}{e^{-2\tau/T_{1R}}} = M_0 \exp\left[-2\tau\left(\frac{^{63}T_1}{^{63}T_{2M}^2} + \frac{^{65}T_1}{^{65}T_{2M}^2} \right) \right], \quad (5)$$

where $^\alpha T_{2M}^{-2} \equiv {}^\alpha\langle \Delta\omega^2 \rangle$ is the contribution from the α-nuclei ($\alpha = 63, 65$) to the second moment of ^{63}Cu, and $^\alpha T_1$ is the spin-lattice relaxation time in the α site. Note that $^{63}T_{2M}$ corresponds to T_{2G} in the static limit. Here, ^{65}Cu also contributes to the ^{63}Cu decay because they lose their memories of the initial states during the echo sequence due to the fluctuation effect, so that

their contributions are not canceled out at the time of the ^{63}Cu echo.

In the present case, the transition from the static to the narrowing regime is caused by the large anisotropies of T_1^{-1} and T_{2M}^{-1}. As will be shown later, T_{2M}^{-1} decreases by 3.3 from $\theta = 0°$ to $90°$, while T_1^{-1} increases by 2.1. Also, there is a qualitative correspondence between the transition of the decay curve in Fig. 2(a) and the simulations by Walstedt *et al.* for the various values of T_1/T_{2M} (Fig. 4 of Ref. [22]). The angular dependence of T_{2M}^{-2} deduced from either T_{2G} or T_{2L} in Fig. 2(c) is shown in Fig. 2(d), where $T_{2M} = T_{2G}$ while Eq. (5) is used to obtain $^{63}T_{2M}$ from T_{2L} along with the relations,

$$(^{63}\gamma)^2 \cdot {}^{63}T_1 = (^{65}\gamma)^2 \cdot {}^{65}T_1, \qquad (6)$$

$$^{65}c \cdot (^{65}\gamma_n \cdot {}^{65}T_{2M})^2 = {}^{63}c \cdot (^{63}\gamma_n \cdot {}^{63}T_{2M})^2, \qquad (7)$$

where $^{\alpha}c$ is the natural abundance for the isotope α.

The angular dependence of T_{2M}^{-2} in Fig. 2(d) is consistent with that of the hyperfine coupling constant. This situation corresponds to the detuned limit, where inhomogeneous broadening of the NMR lines greatly reduces the number of nearby spins that can conserve energy in the mutual spin-flip process. Consequently, the flip-flop terms $(I_i^+ I_j^-)$ in the nuclear Hamiltonian can be discarded [1,25]. Thus, T_{2M}^{-2} is given only by the z component term $(I_i^z I_j^z)$ so that

$$[T_{2M}(\theta)]^{-2} \propto \{F_{\mathbf{Q}}(\theta)\}^2 \cdot \sum_q \chi(\mathbf{q})^2, \qquad (8)$$

where $F_{\mathbf{q}}(\theta)$ is the form factor when H_0 is in the θ direction [2]. Here we assume that the q dependence of $F_{\mathbf{q}}$ around $\mathbf{Q} \equiv (\pi, \pi)$ is weaker than that of $\chi(\mathbf{q})$, so that $F_{\mathbf{q}}$ is represented by $F_{\mathbf{Q}}$ and taken out of the q summation. Since the θ dependence of $F_{\mathbf{Q}}(\theta)$ is $\{A(3\cos^2\theta - 1) + B\}^2$ where A and B are constants, the anisotropy of T_{2M}^{-2} is given by

$$[T_{2M}(\theta)]^{-2}/[T_{2M}(90°)]^{-2} = (\sin^2\theta + \eta \cos^2\theta)^4, \qquad (9)$$

where $\eta \equiv [F_{\mathbf{Q}}(0°)/F_{\mathbf{Q}}(90°)]^{1/2}$. The value of η can be estimated from the anisotropy of T_1^{-1}. Since $\chi(\mathbf{Q}) \gg \chi(0)$ in this system, $(T_1)_z^{-1} \propto \{F_x(\mathbf{Q}) + F_y(\mathbf{Q})\}$ [19]. Hence, η is given by

$$\eta \equiv \left[\frac{F_{\mathbf{Q}}(0°)}{F_{\mathbf{Q}}(90°)} \right]^{1/2} \approx \left[2\frac{[T_1(90°)]^{-1}}{[T_1(0°)]^{-1}} - 1 \right]^{1/2}. \qquad (10)$$

From Fig. 2(b), $[T_1(90°)]^{-1}/[T_1(0°)]^{-1} = 2.1$, so that $\eta = 1.79$. The dashed curve in Fig. 2(d) shows the anisotropy of T_{2M}^{-2} obtained from Eq. (9) with $[T_{2M}(90°)]^{-2}$ as a single adjustable parameter. Even with our simplifying assumptions, it has the same tendency as the angular dependence of T_{2G}^{-2}.

The analysis at $0°$, $10°$, and $70°$ is not straightforward because of the overlap with the Cu(2) line. Since T_{2M}^{-1} at Cu(2) is expected to be smaller than that of Cu(1) by a

factor of 0.75 [19], the overlapped Cu(2) line reduces T_{2M}^{-1}. T_{2M}^{-2}, however, is not reduced at $10°$, and is significantly enhanced at $0°$. At $70°$, the shape of the decay curve itself is quite different from those at $60°$ and $80°$. Below, we show that these features can be attributed to the interlayer spin correlations, which have the effect of enhancing T_{2M}^{-1} [11,12].

Consider the echo decay process at $\theta = 0°$. As seen in Fig. 1, the Cu(1) and Cu(2) lines are situated close to each other, so that not only Cu(1) but also a part of Cu(2) nuclei are excited, which also act as like-spins for the Cu(1) nuclei in the echo decay process. On the other hand, the intensity of the echo is obtained by integrating only the Cu(1) part of the FT spectrum of the echo (shaded part of the spectrum in Fig. 1), so that only the Cu(1) nuclei contribute to the intensity of the decay curve in Fig. 2(a). This is the same situation as that in the double resonance experiment where the π pulses for like- and unlike-spins are applied simultaneously. Since all the like-spins contribute to the Gaussian decay in the static limit, $[T_{2M}(0°)]^{-2}$ is given by [12],

$$[T_{2M}(0°)]^{-2} \propto \sum_q [F_{\mathbf{q}}(0°)\{\chi^{11}(\mathbf{q}) + 4\epsilon\chi^{12}(\mathbf{q})\}]^2, \quad (11)$$

where χ^{11} and χ^{12} are the intralayer and interlayer spin susceptibilities associated with the autocorrelations and cross correlations within or between layers indicated in Fig. 3. The second term in Eq. (11) corresponds to the contribution due to the interlayer correlations. The coefficient "4" reflects the number of neighboring planes (it is "2" in the bilayer systems) [12], and the ratio of the excited Cu(2) nuclei (ϵ) is estimated to be about 0.6.

At the angles where the two Cu lines are separated from each other, the second term in Eq. (11) does not appear in the echo decay process, whereas at $10°$ and $70°$, both the Cu(1) and Cu(2) nuclei are excited and observed, so that the second term in Eq. (11) also appears, which enhances T_{2M}^{-2}. This enhancement increases T_1/T_{2M}, and brings the situation at $70°$ closer to the static limit, resulting in the appearance of the Gaussian component in the decay curve. At $10°$, a cancellation may occur between the reduction due to the overlapped Cu(2)
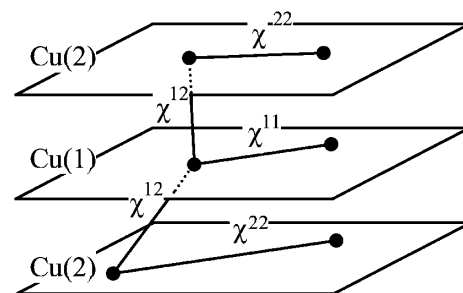
FIG. 3. Schematic view of the intra ($i = j$) and interlayer ($i \neq j$) spin susceptibilities [$\chi^{ij}(\mathbf{q})$] in the trilayer system.
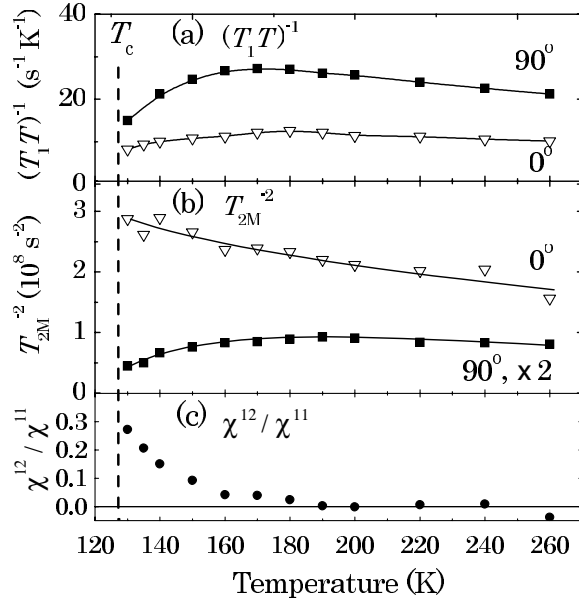
FIG. 4. T dependences of (a) $(T_1T)^{-1}$ and (b) T_{2M}^{-2} at 0° and $2T_{2M}^{-2}$ at 90°. (c) $\chi^{12}(\mathbf{Q})/\chi^{11}(\mathbf{Q})$ defined by Eq. (14).

line and the enhancement due to the interlayer spin correlations.

Figure 4(b) shows the T dependences of T_{2M}^{-2} at 0° and 90°, which are quite different from each other; i.e., while $[T_{2M}(90°)]^{-2}$ starts to decrease at T_{pg} as does $(T_1T)^{-1}$ shown in Fig. 4(a), $[T_{2M}(0°)]^{-2}$ continues to grow down to T_c. This difference is caused by the χ^{12} term in Eq. (11). For simplicity, we assume $\chi^{ij}(\mathbf{q}) \equiv \chi^{ij}(\mathbf{Q})$ for $|\mathbf{q}-\mathbf{Q}| < \xi^{-1}$ and 0 otherwise, where ξ is a correlation length. T_{2M}^{-2} at 0° and 90° can be rewritten as [12,18],

$$[T_{2M}(0°)]^{-2} \propto [F_\mathbf{Q}(0°)\{\chi^{11}(\mathbf{Q}) + 4\epsilon\chi^{12}(\mathbf{Q})\}]^2 \xi^{-2}$$
$$[T_{2M}(90°)]^{-2} \propto \{F_\mathbf{Q}(90°)\chi^{11}(\mathbf{Q})\}^2 \xi^{-2}. \quad (12)$$

Here we define the ratio ρ by

$$\rho \equiv \frac{[T_{2M}(0°)]^{-2}}{[T_{2M}(90°)]^{-2}} \eta^{-4} = \left[1 + 4\epsilon\frac{\chi^{12}(\mathbf{Q})}{\chi^{11}(\mathbf{Q})}\right]^2, \quad (13)$$

which gives

$$\chi^{12}(\mathbf{Q})/\chi^{11}(\mathbf{Q}) = (\sqrt{\rho} - 1)/4\epsilon. \quad (14)$$

The T dependence of $\chi^{12}(\mathbf{Q})/\chi^{11}(\mathbf{Q})$ calculated from ρ is shown in Fig. 4(c), where η is adjusted so that $\rho = 1$ at high T. One can see that $\chi^{12}(\mathbf{Q})/\chi^{11}(\mathbf{Q})$ rapidly increases in the pseudogap T region, indicating that $\chi^{12}(\mathbf{Q})$ rapidly grows there. This is consistent with the SEDOR results [14,15] and the theoretical calculations [12,13,26,27]. Note that $\chi^{12}(\mathbf{Q})/\chi^{11}(\mathbf{Q}) \approx T_{2S}^{-1}/T_{2G}^{-1}$ where T_{2S} is the SEDOR decay time between the sites on the different layers. From Fig. 4(c), we find that $\chi^{12}(\mathbf{Q})/\chi^{11}(\mathbf{Q}) = 0.28$ at T_c, while T_{2S}^{-1}/T_{2G}^{-1} was reported to be about 0.25 at T_c in $Y_2Ba_4Cu_7O_{15}$ [15]. The consistent explan-

ation for both T_{2M}^{-1} and T_{2S}^{-1} indicates that they can be interpreted on the same basis of the interlayer spin correlations.

In conclusion, we have investigated the anisotropy of the spin echo decay in the inner Cu site of the trilayer cuprate $Hg_{0.8}Re_{0.2}Ba_2Ca_2Cu_3O_8$ to obtain the anisotropy of the second moment T_{2M}^{-2}. Comparison between the data at 0° and 90° shows the rapid growth of $\chi^{12}(\mathbf{Q})$ in the pseudogap regime. Since this is a common effect in multilayer systems, we conclude that the opposite T dependences between $(T_1T)^{-1}$ and T_{2G}^{-2} observed in the pseudogap regime of bilayer systems are caused by interlayer spin correlations.

[1] Y. Itoh et al., J. Phys. Soc. Jpn. **61**, 1287 (1992).
[2] M. Takigawa, J. Phys. Chem. Solids **53**, 1651 (1992).
[3] K. Magishi et al., Phys. Rev. B **57**, 11 533 (1998).
[4] M. Itoh et al., Phys. Rev. B **54**, R9631 (1996).
[5] J. Kishine, J. Phys. Soc. Jpn. **66**, 1229 (1997).
[6] T. Moriya, *Spin Fluctuations in Itinerant Electron Magnetism* (Springer-Verlag, Berlin, 1985).
[7] M. U. Ubbens and P. A. Lee, Phys. Rev. B **50**, 438 (1994).
[8] A. J. Millis, H. Monien, and D. Pines, Phys. Rev. B **42**, 167 (1990).
[9] T. Tanamoto, H. Kohno, and H. Fukuyama, J. Phys. Soc. Jpn. **62**, 717 (1993).
[10] Y. Itoh et al., J. Phys. Soc. Jpn. **67**, 312 (1998).
[11] J. Kishine, Thesis, University of Tokyo, 1996.
[12] A. Goto and T. Shimizu, Phys. Rev. B **57**, 7977 (1998).
[13] J. Kishine, Physica (Amsterdam) **282-287C**, 1771 (1997).
[14] R. Stern, M. Mali, J. Roos, and D. Brinkmann, Phys. Rev. B **52**, R15 734 (1995).
[15] A. Suter, M. Mali, J. Roos, and D. Brinkmann, Phys. Rev. Lett. **82**, 1309 (1999).
[16] P. V. P. S. S. Sastry et al., Physica (Amsterdam) **297C**, 223 (1998).
[17] W. G. Clark, M. E. Hanson, F. Lefloch, and P. Ségransan, Rev. Sci. Instrum. **66**, 2453 (1995).
[18] A. Goto, T. Shimizu, P. V. P. S. S. Sastry, and J. Schwartz, Phys. Rev. B **59**, R14 169 (1999).
[19] K. Magishi et al., J. Phys. Soc. Jpn. **64**, 4561 (1995).
[20] M.-H. Julien et al., Phys. Rev. Lett. **76**, 4238 (1996).
[21] A. G. Redfield, IBM J. Res. Dev. **1**, 19 (1957).
[22] R. E. Walstedt and S.-W. Cheong, Phys. Rev. B **51**, 3163 (1995).
[23] A. Abragam, *The Principles of Nuclear Magnetism* (Oxford University Press, New York, 1961).
[24] M. Takigawa and G. Saito, J. Phys. Soc. Jpn. **55**, 1233 (1986).
[25] N. J. Curro et al., Phys. Rev. B **56**, 877 (1997).
[26] H. Monien and T. M. Rice, Physica (Amsterdam) **235-240C**, 1705 (1994).
[27] A. Goto and T. Shimizu, Physica (Amsterdam) **259-261B**, 468 (1999).